

Effects of Fe fine powders doping on hot deformed NdFeB magnets

Min Lin ^{a,*}, Huijie Wang ^b, Jingwu Zheng ^c, Aru Yan ^a

^a Ningbo Institute of Material Technology & Engineering Chinese Academy of Science, Ningbo 315201, People's Republic of China

^b Ningbo Jinji Strong Magnetic Material Company, Ningbo 315041, People's Republic of China

^c Zhejiang University of Technology, Hangzhou 310014, People's Republic of China

ARTICLE INFO

Keywords:

Composite NdFeB magnets

Bending strength

Hot deformed behavior

Corrosion resistance

ABSTRACT

The composite NdFeB magnets with blending melt-spun flakes and Fe fine powders were prepared by the hot-pressed and hot-deformed route. Characterizations of the hot-deformed NdFeB magnets affected by the doped Fe powders were tested. The doped Fe powders decrease the hot-deformed pressure when the strain is between 15 and 50%. XRD patterns show that the doped Fe powders have little influence on the *c*-axis alignment of hot-deformed NdFeB magnets in the press direction. The B_r and the $(BH)_{max}$ get improved when the doped Fe powders are less than 3 wt%. The doped Fe of hot-deformed NdFeB magnets exists in the elongated state and the spherical state surrounded by the Nd-rich phase. With the Fe fraction increasing, the potential of magnet moves to the positive direction and the diameter of the Nyquist arc becomes larger, which indicate that the corrosion resistance improved effectively. The bending strength was enhanced by the elongated α -Fe phase embedded in the matrix 2:14:1 phase.

1. Introduction

NdFeB magnets are widely used in the construction of battery-operated tools, magnetic resonance imaging units, electric bicycles, electric-assisted vehicles, speakers, magnetic separation units, etc. [1]. The hot-pressed/hot-deformed NdFeB magnets have been commercially available for many years [2]. They offer many advantages over the sintered magnets, such as shorter preparing process, more environmental stability, near-net final shapes, and so on [3,4]. However, their mechanical properties such as bending strength and fracture toughness are poor, as compared with their sintered forms [5]. High deformed levels tend to promote cracks, which reduce the density and the B_r . We found the enhanced magnetic properties and bending strength of hot-deformed NdFeB magnets with the fine mixing Cu powders [6].

The melt spun-hot pressed-hot deformed process is a promising method of preparing α -Fe/Nd₂Fe₁₄B nanocomposite magnets [7]. If this kind of magnets want to exhibit the exchange-coupling effect, both α -Fe and Nd₂Fe₁₄B grains need to be less than 10 nm. On the other hand, the calculation also shows that soft magnetic inclusions of any size can be fully magnetically coupled with the hard matrix by long-range magnetostatic interactions provided that the inclusion forms the layer perpendicular to the magnetization direction [8]. The anisotropic hot-pressed magnets

made of the blends of the melt-spun NdFeB ribbons and coarse α -Fe and Fe-Co powders were reported. The composite magnets exhibited a uniform demagnetization behavior and some showed the enhanced values of the B_r and $(BH)_{max}$ [9]. However, if this kind of magnets wants to put into practical service, more characterizations need to be investigated, such as the hot deformed process, the mechanical properties and the corrosion behavior, and so on. In this paper we doped the hot-deformed NdFeB magnets with the Fe fine powders. The change of magnetic properties and other characterizations were analyzed.

2. Experiments

The magnetic alloys with composition Nd_{13.5}Fe₈₀Ga_{0.5}B₆ were prepared by induction melting. Melt spinning was then used to make ribbons with a wheel speed 40–50 m/s. The ribbons were crushed into about 500 μ m powders. The melt-spun powders with and without Fe powders were mixed with a 3-dimension movement blender. In vacuum they were hot-pressed at 600–800 °C under 100–200 MPa. Then they were hot-deformed at 700–900 °C under 80–150 MPa. The specimens were reduced to the 40% of their original thickness.

The magnetic properties were measured with a NIM-2000 hysteresis loop tracer. The alignment in the press direction was analyzed with a Bruker Discover X-ray diffraction (XRD). The morphology of the magnet was observed with a FEI Quanta 250

* Corresponding author.

E-mail address: linm@nimte.ac.cn (M. Lin).

Scanning Electron Microscope (SEM). Bending strength was measured by a 3-point bend test with a span of 14.5 mm in an Instron 5567. The specimen was a $5 \times 6 \times 19 \text{ mm}^3$ magnet with the easy axis perpendicular to the load direction. Corrosion properties were tested through potentiodynamic polarization and electrochemical impedance spectroscopy (EIS). The three-electrode method was applied, with the tested sample as the working electrode, a saturated calomel electrode (SCE) as the reference and a platinum plate as the counter electrode. Measurement was taken in 3.5 wt% NaCl solution at room temperature. The working electrode was with an approximate transversal area of 25 mm^2 . The EIS was tested at open-circuit potential (OCP) with a M273 model potentiostat and M5210 model lock-in amplifier. The amplitude of perturbation signals was 10 mV, and the frequency ranged from 10^{-2} to 10^5 Hz with an acquisition rate of 7 points per decade. Potentiodynamic polarization was measured with a CH Instruments Model 660A electrochemical analyzer/workstation at the 0.2 mV/s scanning rate.

3. Result and discussion

The micrograph of the Fe powders we used is shown in Fig. 1. Most of them are fine and well distributed. The particle sizes are ranging from 15 to $40 \mu\text{m}$ tested by a Helos H2365 particle size analysis.

The pressure and strain of the Fe-free and Fe-doped samples are recorded per second in the hot-deformed process, as shown in Fig. 2. The flow stresses show almost a flat step when the deformed processes are less than 50%. For the whole 65% strain it needs higher flow stress in the deformed process completion. The doped Fe powders decrease the pressure when the strain is between 15 and 50%. However, the pressure increased a little when the strain is beyond 50%.

We measured the alignment of the Fe-free and Fe-doped samples by the ratio of $B_{r\parallel}$ and $B_{r\perp}$, which was only a little different (less than 5%). The XRD patterns of the Fe-free and Fe-doped samples (3 and 7 wt%) in the press direction are shown in Fig. 3. A better grain alignment is represented by enhanced (004), (006), and (008) intensities and a greater than 1 intensity ratio of (006) over (105) [9]. According to this experience rule, we calculated the ratio of (006) over (105) and the ratio of $\Sigma(00i)(i=4, 6, 8)$ over (105) of the samples. It is found that the doped Fe particles have little influence on the c -axis alignment of the magnetic main phase

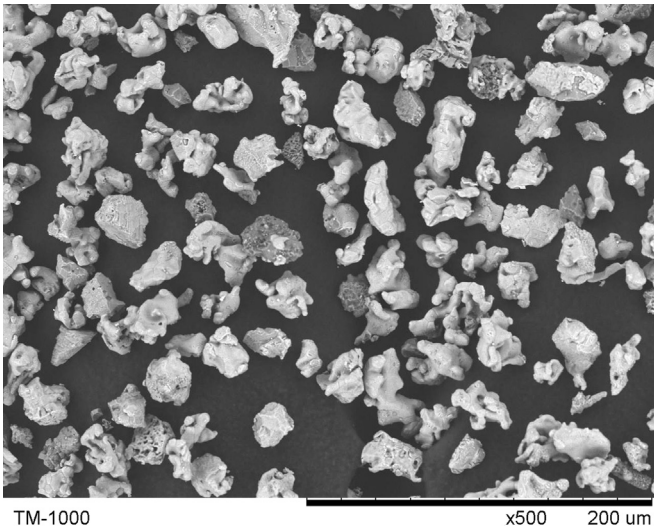


Fig. 1. Micrograph of the Fe powders used in this work.

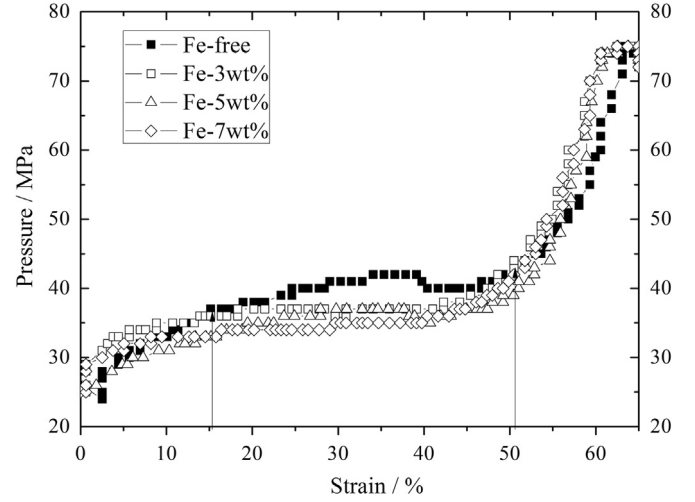


Fig. 2. Pressure and strain of the Fe-free and Fe-doped samples in the hot-deformed process.

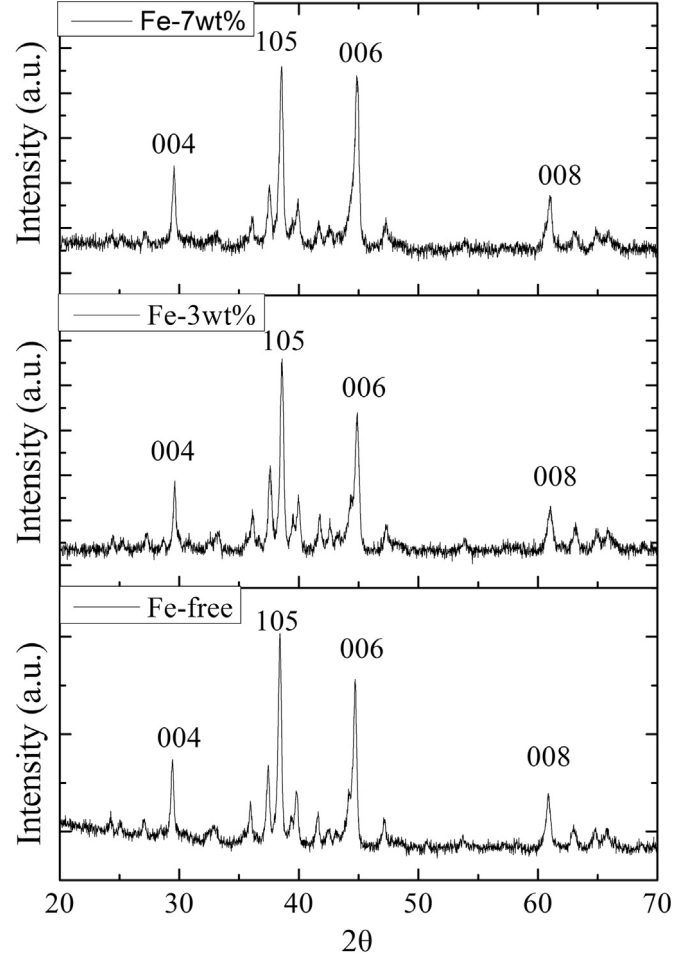


Fig. 3. XRD patterns of the Fe-free and Fe-doped samples in the press direction.

in the press direction.

The magnetic properties of the Fe-free and Fe-doped samples are shown in Fig. 4(a). The addition of soft phase resulted in higher magnetization but lower coercivity. With the increasing Fe fraction, the H_{c1} always decreases but the B_r and $(BH)_{\max}$ get improved when the Fe fraction was less than 3%. The change of magnetic properties before and after the 3 wt% Fe-doped is shown in Fig. 4(b). It is shown that both the B_r and $(BH)_{\max}$ get improved,

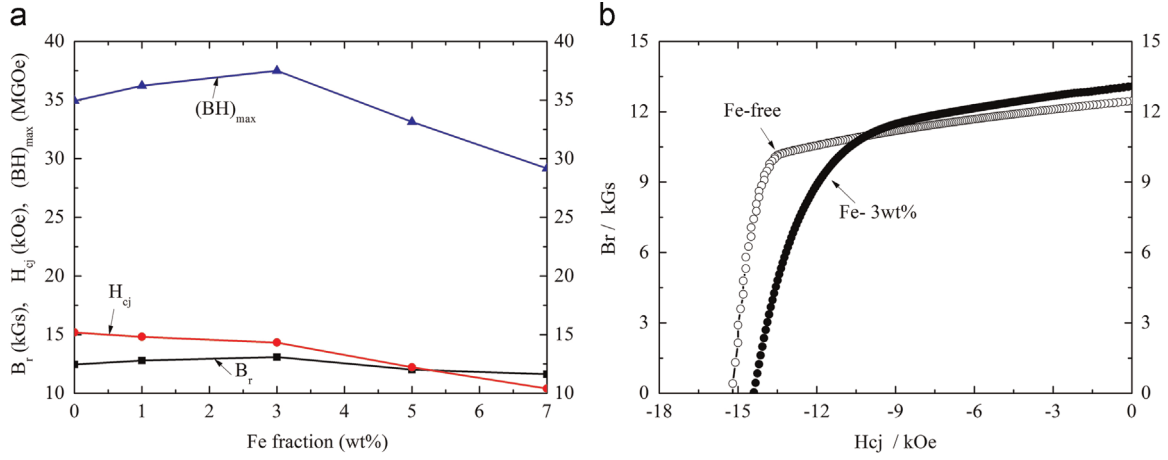


Fig. 4. Effects of Fe fraction on magnetic properties of the Fe-free and Fe-doped samples (a) and demagnetization curves (b).

increasing from 12.46 kOe to 13.09 kOe and from 34.93 MGOe to 37.62 MGOe respectively. The H_{cj} and the squareness slightly decreased. The improved B_r and $(BH)_{max}$ may arise from the magnetic coupling between the hard matrix phase and the soft α -Fe flakes by the long-range magnetostatic interactions[8].

The density of Fe-doped samples were measured with

Archimedes drainage method, which showed that they were no porosity. Fig. 5 is the backscattered scanning electron image of the polished surface of the Fe-free and Fe-doped samples. The dark gray phase is the α -Fe, while the light gray is the 2:14:1 phase. The microstructure of the Fe-free sample is shown in Fig. 5(a), where small grains exist between coarse large grains. After Fe powders

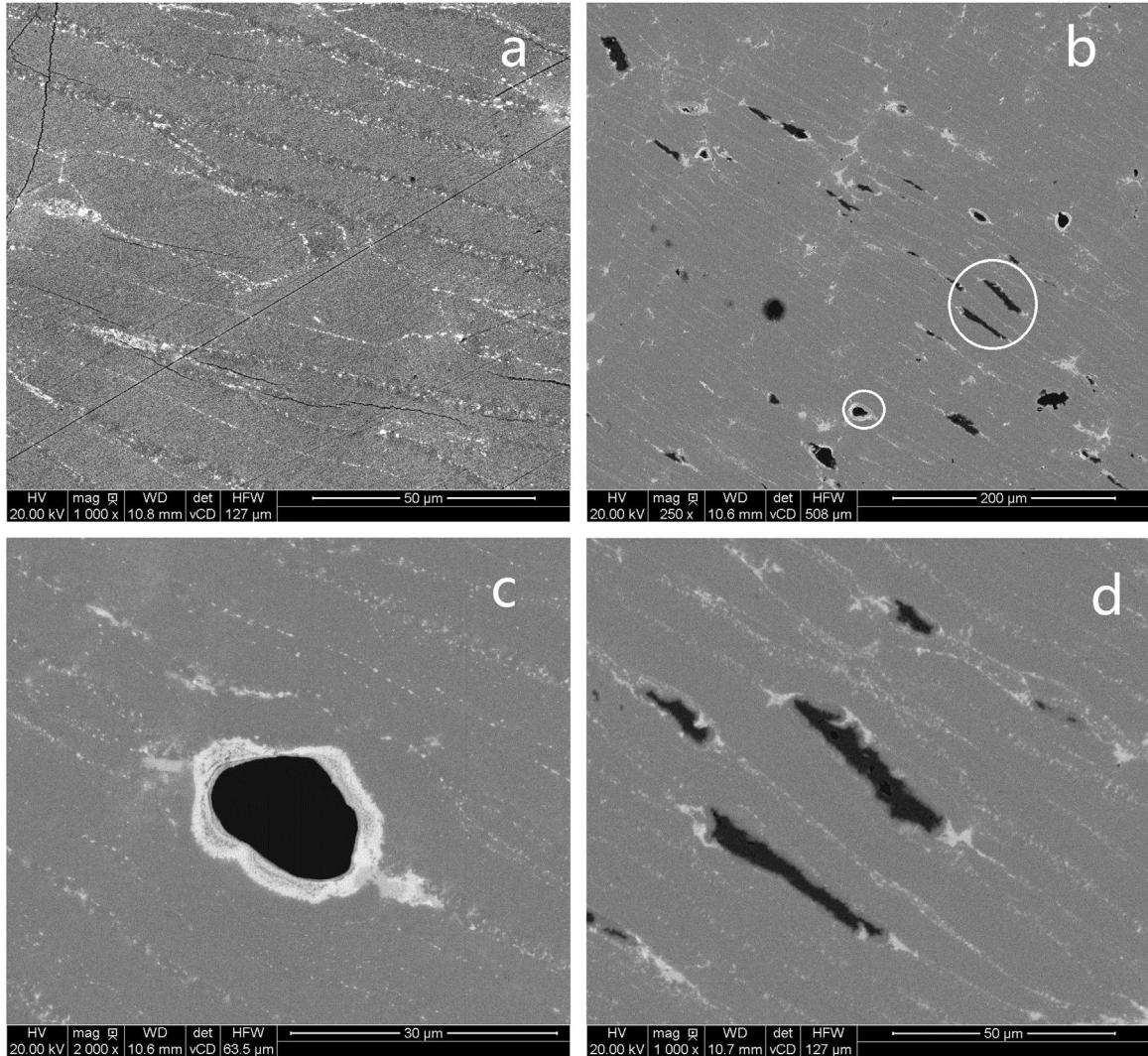


Fig. 5. SEM images of the polished surface of the Fe-free (a) and Fe-doped (b-d) samples.

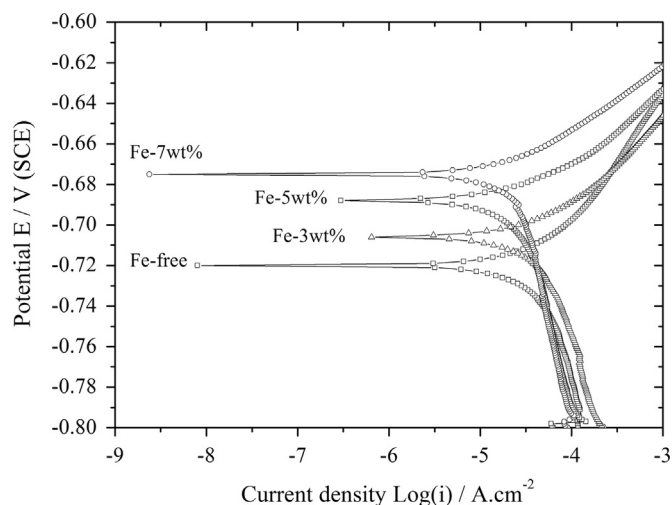


Fig. 6. Potentiodynamic polarization curves of the Fe-free and Fe-doped samples.

are doped, the microstructure of the sample changes as shown in Fig. 5(b–d). Fig. 5(c) and (d) shows an enlarged image of the encircled region in Fig. 5(b). Apparently, two shapes of Fe particles in Fe-doped samples were distributed evenly, as shown in Fig. 5b. One is that the appearance of the Fe powder is similar to the original spherical particle, surrounded by the Nd-rich phase, as shown in Fig. 5(c). The other is that the Fe powder has a length of up to over 50 μm and a thickness of 10–20 μm , as shown in Fig. 5 (d). The Fe powders are elongated perpendicular to the press direction, which may be the reason that the samples with Fe-doped consume more pressure in the final hot-deformed process as shown in Fig. 2. Generally the Fe particles in elongated shape were more than the Fe particles in spherical shape.

The potentiodynamic polarization curves of the Fe-free and Fe-doped samples in 3.5% NaCl solution are shown in Fig. 6. The corrosion potential of the hot-deformed NdFeB magnet moves positively from -0.72 to -0.67 V and its current density becomes smaller, which indicates that the thermodynamic stability is improved and its corrosion resistance becomes better. Besides, the color of the solution-dissolved Fe-doped samples is green, which is different from the yellow color of the Fe-free samples. It may illustrate the cathodic protection function for the hot-deformed NdFeB magnet because of the prior Fe-doped dissolution.

The Nyquist plots of the Fe-free and Fe-doped samples in 3.5% NaCl solution are shown in Fig. 7. They present different EIS characteristics. All of the Nyquist curves have two capacitance loops. The capacitance loop at high frequency corresponds to the electrochemical process while the capacitance loop at low frequency corresponds to the mass transferring process. All of the diameters of the Nyquist arcs of the Fe-doped samples are larger than that of the Fe-free sample. It indicates that the corrosion resistance of the Fe-doped samples improved effectively, which is in accordance with Fig. 6.

The mechanical tests were repeated seven times in order to obtain average values. The deviation of maximum fracture strength was 5%. The mechanical test shows that the Fe doped samples help to improve the bending strength from 210 to 240 MPa and the strain percentage also increases, shown in Fig. 8. For the Fe-doped magnet, the protruding α -Fe phase can be clearly detected on the fracture surface. It can also be found that the Fe particles were coated by the matrix 2:14:1 phase, shown in Fig. 9, which indicate that the binding between the matrix phase and the α -Fe particles was stronger than that between the matrix particles.

The normal stress of an arbitrary spot in transverse section is directly proportional to its distance from the impartial axis.

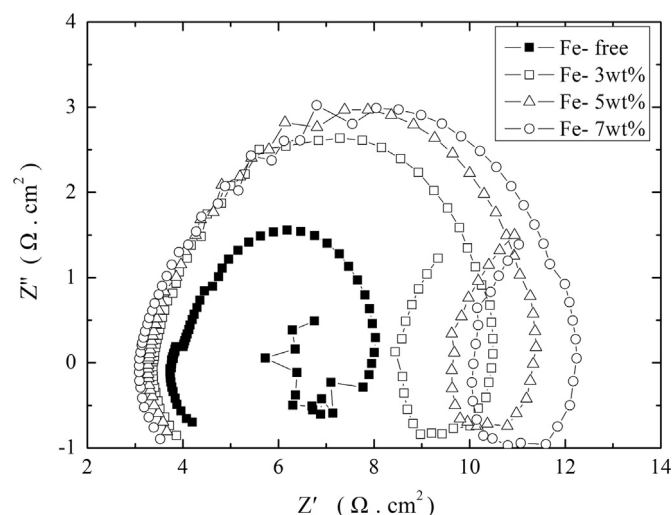


Fig. 7. Nyquist plots of the Fe-free and Fe-doped samples.

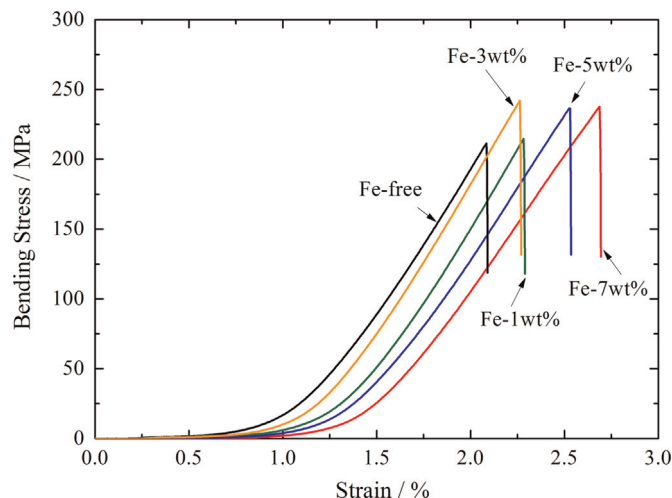


Fig. 8. Bending true stress-strain curves of the Fe-free and the Fe doped hot-deformed magnet.

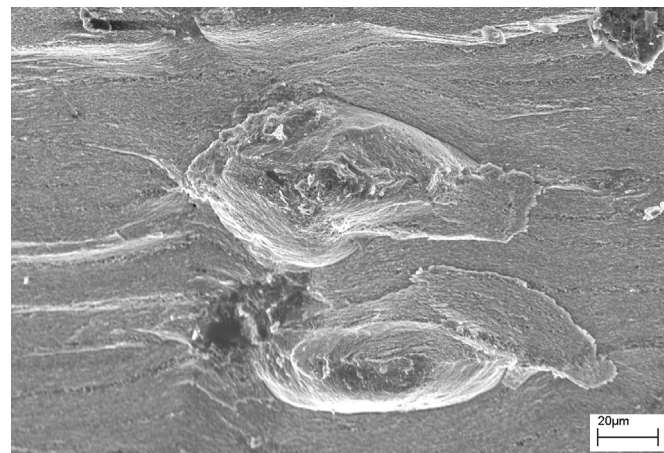


Fig. 9. Morphology of the fracture surface of the Fe doped hot-deformed magnet.

Bending strength is the biggest tensile stress achieved when the tensile area fracture because of the tensile stress is much lower than compressive stress in NdFeB magnets. When fracture occurs, a crack tip is located in the tensile area all the time. The crack tip moves and propagates through the whole specimen. When the

crack is propagating, it is deflected when touching the elongated α -Fe phase. Another effect is that the elongated α -Fe particles will be extracted from the matrix phase and consume the fracture energy. Both of these may account for the improvement of the bending strength.

As for the Fe-doped hot-deformed NdFeB magnets, the altered deformation process may help to suppress the grain growth at the NdFeB flake boundaries. When an increasing compressive stress is applied, plastic deformation occurs in the flakes. Previous study reported the addition of internal lubricant to produce the hot-deformed magnets [10]. The low-melting lubricants help to decrease the friction between the particles, improve the formability during the hot-working step and make the uniformly plastically deformed grains through the products. The plastic deformation Fe particles during die upset may help to decrease the friction between the flakes and have effects similar to the low melting additions.

However, the effect of grain growth suppression by the doped Fe particles still needs further research. The microstructural change on the flake boundary may be another reason for the improvement of bending strength by the doped Fe particle. The further optimization of the grain size of the soft phase would lead to an increase in both the magnetic properties and mechanical properties.

4. Conclusions

The doped Fe powders have little influence on the c-axis alignment of hot-deformed NdFeB magnets in the press direction. With less than 3 wt% Fe powder doped, the B_r and the $(BH)_{\max}$ of hot-deformed NdFeB magnets get improved, while the H_{cj} always decreases. Surrounded by the Nd-rich phase, the doped Fe powders are in spherical state firstly. Then they are hot deformed to

the elongated state. The bending strength was enhanced by the elongated α -Fe phase embedded in the matrix 2:14:1 phase. With the fraction of Fe powder increasing, the potential of magnet moves to the positive direction and the diameter of the Nyquist arc becomes larger, which indicate that the corrosion resistance improved effectively.

Acknowledgements

This work was sponsored by Natural Science Foundation of China Ningbo (Grant no. 2014A610167) and Technology Innovation & Achievement Industrialization Project of China Ningbo (Grant no. 2014B11010).

References

- [1] O. Gutfleisch, M.A. Willard, E. Bruck, C.H. Chen, S.G. Sankar, J.P. Liu, *Adv. Mater.* 23 (2011) 821.
- [2] R.W. Lee, *Appl. Phys. Lett.* 46 (1985) 790.
- [3] B.M. Ma, D. Lee, B. Smith, S. Gaiffi, B. Owens, H. Bie, G.W. Warren, *IEEE Trans. Magn.* 37 (2001) 2477.
- [4] A.A. El-Moneim, O. Gutfleisch, A. Plotnikov, A. Gebert, J. Magn. Magn. Mater. 248 (2002) 121.
- [5] D. Hinz, A. Kirchner, D.N. Brown, B.M. Ma, O. Gutfleisch, J. Mater. Process. Technol. 135 (2003) 358.
- [6] Pengpeng Yi, Min Lin, Renjie Chen, Don Lee, Aru Yan, J. Alloy. Compd. 491 (2009) 605.
- [7] T. Ohkubo, T. Miyoshi, S. Hirose, K. Hono, *Mater. Sci. Eng. A* 449 (2007) 435.
- [8] A.M. Gabay, G.C. Hadjipanayis, *J. Appl. Phys.* 101 (2007) 09K507.
- [9] D. Lee, S. Bauser, A. Higgins, C. Chen, S. Liu, M.Q. Huang, Y.G. Peng, D. E. Laughlin, *J. Appl. Phys.* 99 (2006) 08B516.
- [10] Iwasaki Katsunori, Tanigawa Shigeo, Tokunaga Masuaki, European Patent 89119269.2, 1990.